

# Evaluation of corrosion inhibitors performance using real-time monitoring methods

W. Villamizar-Suárez · J. M. Malo ·

A. Martínez-Villafañe · J. G. Chacon-Nava

Received: 5 December 2009 / Accepted: 4 July 2011 / Published online: 17 July 2011  
© Springer Science+Business Media B.V. 2011

**Abstract** The implementation of real-time corrosion-monitoring techniques can provide a reliable mechanism for detecting the overall effectiveness of chemical treatment programs and contribute to the selection and implementation of an adequate corrosion inhibitor system. Inadequate corrosion monitoring can result in an increase of both uniform and localized (pitting) corrosion activities which can lead to premature material failures. The present research was undertaken to ascertain whether linear polarization resistance (LPR), harmonic analysis (HA), and electrochemical noise (EN) in combination are suitable for the study of performance of corrosion inhibitors under a wide variety of conditions; for example, in the absence and the presence of hydrocarbons with or without the addition of corrosion inhibitors. The findings showed questionable results regarding the usefulness of the pitting factor derived from EN and HA data. In addition, statistical parameters were obtained, such as skew and kurtosis, and these results were compared with the pitting factor.

**Keywords** Inhibitors · Electrochemical noise · Harmonic analysis · On-line monitoring · Pitting factor · Skew · Kurtosis

## 1 Introduction

Over the last decade, the availability of a wide-range of electrochemical techniques and associated equipment provides the present day corrosion engineers with the means to monitor corrosion on-line and in real-time, which were unimaginable just a few years ago. The injection of corrosion inhibitors is a standard practice in oil and gas production systems to control internal corrosion of carbon steel structures. This strategy has shown to be a very successful and cost effective procedure [1]. The selection of chemical treatments for a specific application field would typically undergo a rigorously programmed analysis, followed by a technical field assessment. A traditional and widely accepted standard of corrosion monitoring is the evaluation of corrosion coupons. This method provides adequate information on average mass loss rates and identifies the extent and distribution of corrosion. However, one of the biggest drawbacks with regard to this method is that it only provides time average data and it cannot be used for real-time or on-line corrosion monitoring. The importance of on-line corrosion monitoring is recognized because a large number of electrochemical techniques are being adopted, and other new techniques are being explored as well. After the coupon method, the most accepted techniques for the assessment of corrosion monitoring behavior are usually linear polarization resistance (LPR) and electrical resistance (ER) methods [2]. It is recognized that, there are limitations in the selection of chemicals simply on the basis of LPR results.

---

W. Villamizar-Suárez · A. Martínez-Villafañe ·  
J. G. Chacon-Nava (✉)  
Centro de Investigación en Materiales Avanzados,  
S.C. Miguel de Cervantes 120, Complejo Industrial Chihuahua,  
CP 31109 Chihuahua, Chih, Mexico  
e-mail: jose.chacon@cimav.edu.mx

W. Villamizar-Suárez  
Instituto Colombiano del Petroleo, 45A, Piedecuesta,  
Santander, Colombia

J. M. Malo  
Instituto de Investigaciones Eléctricas, Reforma 113,  
Col. Palmira Temixco, Morelos 62490, Mexico

Wider possibilities of chemical selection are provided by the use of electrochemical techniques based on nonlinear measurements. Harmonic analysis (HA) is based on perturbation with AC signal and the analysis of the nonlinear response in the frequency domain. This allows for the extraction of the required kinetic parameters from the corrosion process. The analysis of the harmonics of the current response affords the possibility of obtaining the corrosion rate and both the anodic and the cathodic Tafel parameters within one measurement [3]. HA and LPR techniques perform well in aqueous-conducting environments, when general corrosion is occurring. The main advantage of HA is that the measurement of the corrosion rate does not employ presumed or estimated values from Tafel slopes. Measurements can be performed in a fraction of time in comparison with conventional methods. HA has been applied in various studies of corrosion and under a variety of conditions [4–6]. Electrochemical noise (EN) performs well not only in aqueous environments, but also in mixed phases like hydrocarbon and low conductivity environments, in either stable or unstable conditions. EN monitoring obtains real-time corrosion data, which provides information of both the level of corrosion activity for a particular system and the dominant corrosion mechanism [7–9]. Thus, EN can be used for screening and efficiency evaluation of corrosion inhibitors, and for the optimization of the injection rates (batch or continuous) [10, 11]. The pitting factor and higher order statistical measures (skew and kurtosis) are potentially applicable for corrosion monitoring. Papavinasam et al. [12] obtained information on pitting corrosion by using three methods: pitting index, pitting factor, and pit indicator. Their results indicated that the correlation between pit indicator and observed pits was higher than those between pitting index and pitting function. The coefficient of current variation (CV) and localization index (LI) have been experimentally related to corrosion mechanism, with large values of CV and/or LI being suggested as indicators of localized corrosion, although these parameters have serious theoretical limitations [13, 14]. More recently, Sanchez-Amaya et al. reported that neither the CV nor the LI could distinguish properly between the different corrosion mechanisms [15]. Barr et al. [11] found a good correlation between kurtosis values and inhibitor concentration. However, further research is necessary to clarify the significance of these parameters. Although electrochemical techniques such as EN and HA continue to gain wider acceptance within the corrosion monitoring and plant operation communities, deeper analysis and interpretation of obtained results from the electrochemical techniques are needed to acquire a better understanding of the corrosion parameters significance.

The present research was carried out to ascertain whether the combination of LPR, HA, and EN and statistical parameters such as skew and kurtosis are suitable for the study of corrosion inhibitors, performance in various conditions, i.e., in the absence and the presence of hydrocarbons in brine solutions.

## 2 Experimental procedure

In this study, corrosion-monitoring analysis was conducted using real-time multi-technique electrochemical corrosion measurement equipment (SmartCET™).<sup>1</sup> The instrumentation applies an automated data acquisition sequence using three electrochemical corrosion measurement techniques (LPR, HA, and EN) and also provides parameters which describe the rate and the mode of the corrosion processes in real operating environments.

LPR may be measured by a number of methods. Typically, LPR monitoring involves the measurement of the polarization resistance,  $R_p$ , of a corroding electrode using small amplitude ( $\approx 25$  mV) sinusoidal polarization of the electrode. For such a relatively small amplitude voltage, Meszaros et al. suggest that the expected error in corresponding HA measurements is about 10% [4]. The slope of the potential/current sweep is measured to provide the polarization resistance, which is inversely proportional to the corrosion current density. Stern and Geary [16] noted that the voltage–current response of the corroding electrode tends to be linear over a small range of potential at either side of the free corrosion potential. The B value is generally taken to be in the range of 26–30 mV for most metal/environment systems and is regarded by most suppliers of LPR instrumentation to be a constant; this parameter is configured into the instrument at the factory. However, the B value is not a constant value for all systems and can vary even within a system subject to changes, i.e., changes in temperature, flow, chemistry in the case of chemical processes and chemical treatment, and so on. Ideally, for accurate corrosion rate measurements, a variable B value should be used.

The HA is a measure of the nonlinear current distortion, arising during the LPR measurement. The HA uses 10 mHz sine wave (50 mV peak-to-peak) and analyzes for current signals at 10, 20, and 30 mHz. The HA technique is capable of determining a corrosion current from the harmonic currents, along with Tafel slopes, allowing for a reliable determination of the corrosion rate, as opposed to LPR that often employs assumed values for the Tafel slopes [6]. In order to provide a measurement of the corrosion current, and to provide an on-line calculation of the

<sup>1</sup> SmartCET™ is a trade mark of Intecorr International, Inc.

Tafel and Stern-Geary constants, the data are analyzed using fast Fourier transform analysis.

The EN refers to the fluctuations in current and potential that occurs on the surface of a metal at free corrosion potential. A parameter known as pitting factor (PF) was derived from EN and HA data. Typically, it has a value between zero and one. As the value approaches one, the system will get into a pitting regime. However, when values approach zero, the system falls into a uniform corrosion regime. PF is defined as [17]:

$$PF = (i_{EN}) / (A_{WE} i_{HA}) \quad (1)$$

where  $i_{EN}$  is the standard deviation of current (determined by EN),  $A_{WE}$  is the electrode surface area,  $\text{cm}^2$ , and  $i_{HA}$  is the corrosion current density from harmonic analysis,  $\text{A}/\text{cm}^2$

## 2.1 Electrodes

All the electrochemical corrosion tests were performed using a three-identical-electrode arrangement each one with  $\sim 9 \text{ cm}^2$  of area. All the electrodes were made of 1018 mild steel. Before testing, the electrodes were abraded with 600 silicon carbide grit paper, and then cleaned with alcohol and acetone, followed by rinsing with distilled water, and drying under a stream of hot air.

## 2.2 Test solutions

Six types of commercial imidazolines as corrosion inhibitors were used in this study (see Table 1). The inhibitors are as follows: hydroxyethyl imidazolines (HEI-18I, HEI-12, and HEI-18), amino-ethyl imidazolines (AEI-18a and AEI-18b), and amido-ethyl imidazoline (AMEI-18) procured from Lakeland Laboratories, UK. The inhibitors were dissolved in a 10% v/v 2-propanol solution, and the inhibitor concentration used was 20 ppm, in all cases.

For the sake of comparison, two solutions were used: solution S1, which is a 3 wt% NaCl aqueous solution, and solution S2 which is a mixture of 90 vol% of the solution S1 plus 10 vol% diesel. The solutions were saturated with  $\text{CO}_2$  for 2 h before testing and kept under a  $\text{CO}_2$  atmosphere during testing. For the experiments, the cell temperature was kept constant at  $50 \pm 2^\circ\text{C}$ . The pH of both the solutions was = 4.2. The solutions were stirred continuously. The working electrode was kept in the electrolyte for 2 h before any inhibitor containing the solution was introduced. A scanning electron microscope (SEM) JEOL JSM-6400 was also employed to observe the surface morphology on selected specimens.

## 3 Results and discussion

### 3.1 LPR/HA results

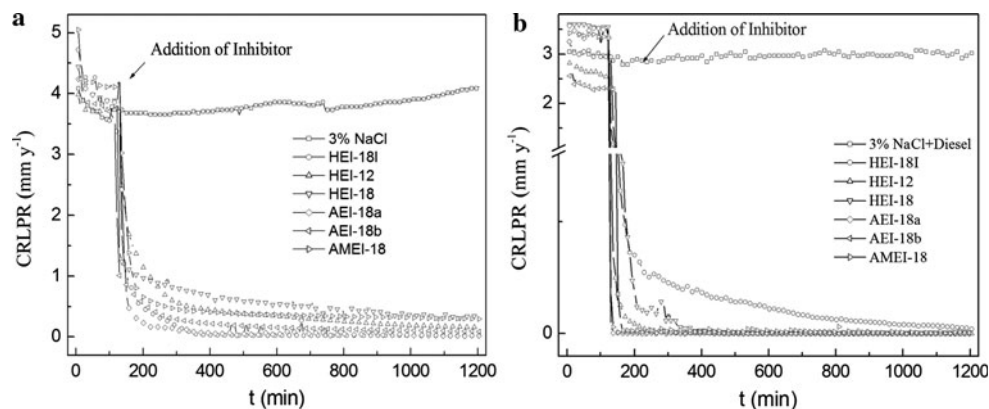
Figure 1a and b shows the variations in corrosion rate, CR, estimated from LPR data with time for electrodes exposed to the solutions S1 and S2 plus the various inhibitors, respectively. In both cases, after 2 h of exposure, the inhibitors were added. real-time monitoring was carried out for 1,200 min (20 h). For the solution S1 plus inhibitors, Fig. 1a shows that the corrosion rates fall rapidly within the first 5–20 min after the inhibitors were added. After the first 20 min, the corrosion rates decrease slowly in an exponential form and after 1,200 min, the corrosion rate is minute (approaching zero) for the AEI-18a, AEI-18b, and HEI-18I inhibitors and with a value of about 0.375 mm/year in the case of HEI-18 and AMEI-18 inhibitors.

Interestingly enough, the HEI-12 hydroxyethyl imidazoline is the most hydrophilic of all the evaluated molecules. Its efficiency was not the best in solution S1. This might indicate the influence of the carbon chain for this kind of molecule as reported previously [18]. It can also be noted

**Table 1** Various imidazoline types used in the present study

Product	Chemical name	Alkyl chain (derivative)
Hydroxyethyl imidazolines		
HEI-18I	1H-imidazole-1-ethanol,4,5-dihydro,-2-C <sub>15-17</sub> unsaturated alkyl derivatives	C <sub>17</sub> (tall oil)
HEI-12	1H-imidazole-1ethanol,4,5-dihydro,-2-nor coco alkyl derivatives	C <sub>12</sub> (cocunut)
HEI-18	1H-imidazole-1ethanol,2-heptadecyl-4,5-dihydro	C <sub>17</sub> (stearic)
Aminoethyl imidazolines		
AEI-18a	Fatty acids, tall oil compounds with diethylene triamine tall oil fatty acid reactions products	C <sub>17</sub> (tall oil)
AEI-18b	Fatty acids, tall oil reactions products compounds with diethylene triamine	C <sub>17</sub> (tall oil)
Amidoethyl imidazolines		
AMEI-18	9-Octadecenamide N-[2-[2-[(8-heptadecenyl)4,5-dihydro-1H-imidazole-1-Y]ethyl-]	C <sub>17</sub> (tall oil)

**Fig. 1** Variations of corrosion rate as determined by LPR measurements with time for 1018 carbon steel exposed to **a** 3% NaCl, and **b** 3% NaCl + diesel solution with the different types of imidazolines



that only in solution S1, the CR remains stable most of the time with a slight tendency to increase at above about 1,000 min.

The presence of an oil phase (solution S2) produced a dramatic and sharp decrease in CR after the addition of the inhibitors in comparison with solution S1, as seen in Fig. 1a and b. In solution S2 plus inhibitors, CR values decreased below 0.025 mm/year: 7 min after the addition of the inhibitor in the case of AEI-18a, after 14 min for AMEI-18's, and after 21 min for the inhibitor AEI-18b. In this case, it is important to note that the SmarCET<sup>TM</sup> equipment takes data cycle readings every 7 min. Because the HEI-18I, HEI-12, and HEI-18 compounds are the most hydrophilic of the various imidazolines used, it takes more time to obtain CR values below 0.025 mm/year.

Figure 2a and b shows the variations in corrosion rate, CR, estimated from HA data with time for electrodes exposed to solutions S1 and S2 plus the various inhibitors, respectively. The corrosion rates obtained by the HA technique followed a similar trend to those obtained by LPR, although these can appear noisy. It is important to observe that the CR values estimated from HA are generally less than half of the obtained values by LPR. The calculation was made by using estimated values of anodic and cathodic Tafel slopes, obtained from the HA technique

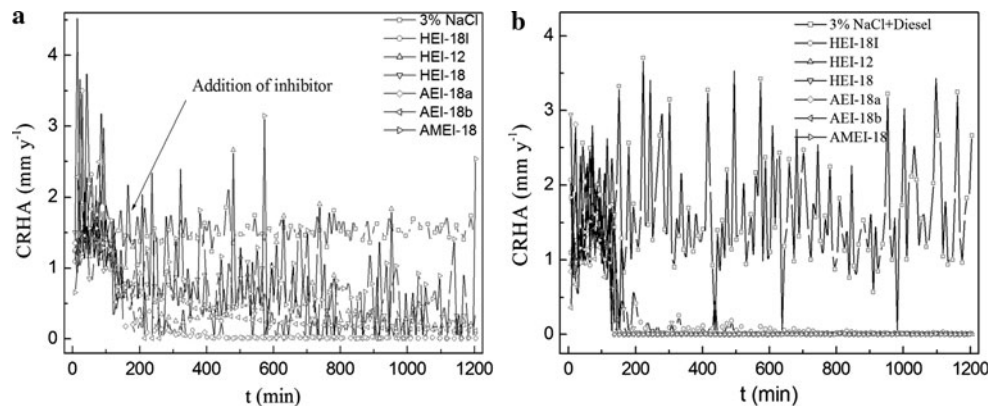
in online analysis. In order to make the calculation of CR from LPR measurements, predetermined anodic and cathodic Tafel slopes of 120 mV value were used.

The results demonstrated an interaction of the hydrocarbon phase with the inhibitor film, improving the hydrophobic properties and the adhesion of this inhibitor film, as demonstrated with measurements of electrochemical impedance spectroscopy by Villamizar et al. [19, 20]. It is worthy to note that the addition of the imidazolines into the oil phase tends to produce a dispersion of the brine–oil mixture because of the surfactant properties of these type of molecules; perhaps being lemulified hydrocarbon-inhibitor drops, instead of being desorbed and divided in the oil phase, they were adsorbed on the metallic surface.

### 3.2 PF from EN and HA measurements

Figures 3 and 4 show the PF obtained from EN and HA data for solutions S1 and S2 plus the addition of the various inhibitors, respectively. During the first few minutes after immersion of the electrodes in both solutions without inhibitors, PF values in the range of 0.01–0.001 were recorded, and these values decreased with time to constant values below 0.001 after 30-min immersion. According to

**Fig. 2** Variation of corrosion rate as determined by HA measurements with time for 1018 carbon steel exposed to **a** 3% NaCl, and **b** 3% NaCl + diesel solution with the different types of imidazolines



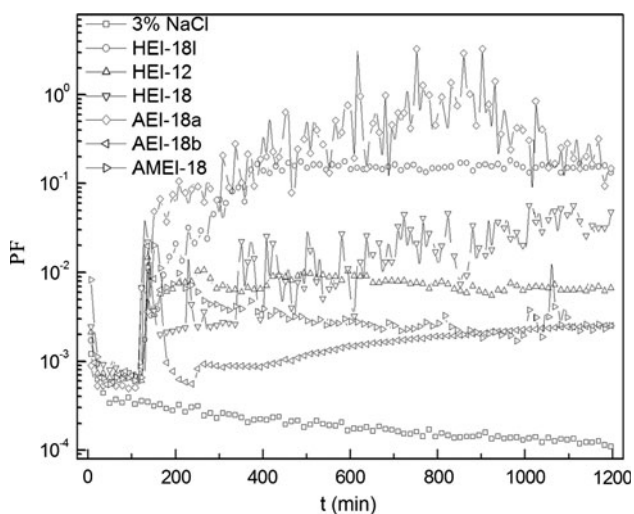


**Fig. 3** Analysis of PF data with time for 1018 carbon steel exposed to 3% NaCl solution with different types of imidazolines

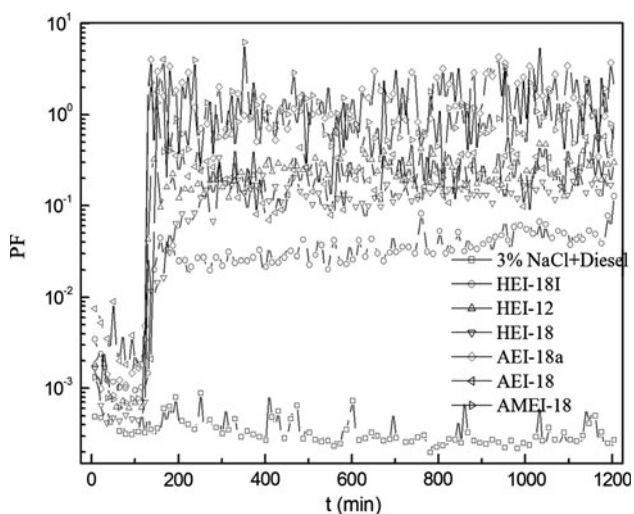


**Fig. 4** Analysis of PF data with time for 1018 carbon steel exposed to 3% NaCl + diesel solution with different types of imidazolines

the literature [21], these PF values correspond to a general corrosion mechanism. However, during the first few minutes after the addition of inhibitors, the PF values showed a sharp increment, reaching greater values than those obtained only for the solutions S1 and S2, as are depicted in Figs. 3 and 4, respectively. In the solution S1 and shortly after addition, only the inhibitors HEI-18I and AEI-18a showed PF values greater than 0.1. For the solution S2, the addition of inhibitors produced an increment of the PF values in the range of 0.1–5, with the exception of the hydroxyethyl imidazoline HEI-18I, for which values below 0.1 were recorded. Overall, the addition of various types of imidazolines produced an increase in PF values. It is particularly interesting to note that in the solution S1, the addition of the AEI-18a inhibitor gave PF values closely to

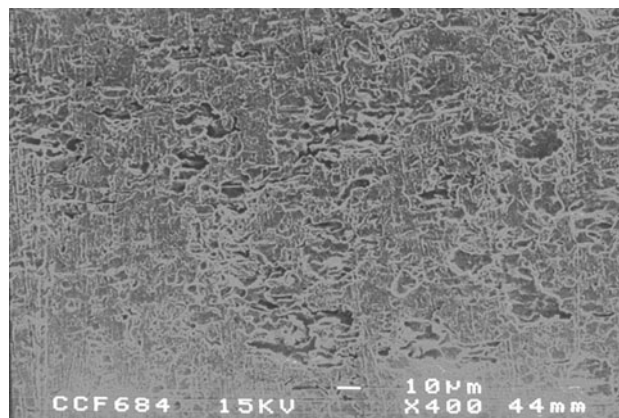


**Fig. 5** SEM micrograph in plan of the surface of a specimen after exposure to 3% NaCl solution with AEI-18a inhibitor

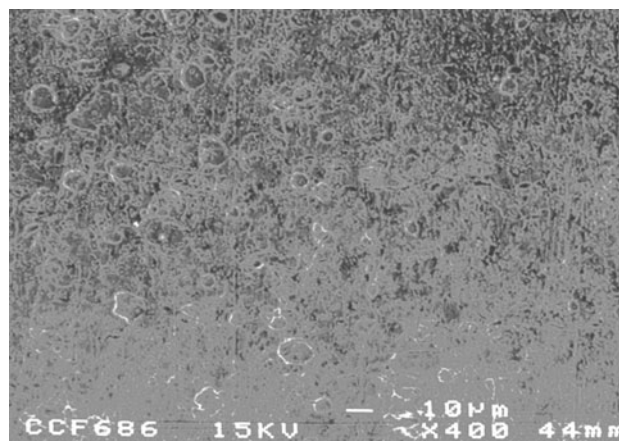


**Fig. 6** SEM micrograph in plan of the surface of a specimen after exposure to 3% NaCl + diesel solution with AEI-18a inhibitor

and above one, from 600 min to 1,000 min of monitoring time. These PF values suggested that, a pitting-like process might be occurring at the electrode surface. A similar observation can be noted for compounds AEI-18a and AMEI-18 added to the solution S2. Thus, to assess the possibility of finding localized corrosion at the surface of the electrodes at the end of the monitoring time, specimens exposed to the aforementioned inhibitors in both the solutions were observed under the scanning electron microscope. No evidence of localized corrosion could be observed, seen in Figs. 5 and 6. Thus, the following question arises: Why do the values of PF approach to a value of one and above? Two possible explanations for this could be: (1) because HA measurements are quite noisy under these conditions, and (2) the corrosion currents are too low, or fluctuate around zero. In such a case, the PF values would erroneously indicate a localized corrosion process. Therefore, special care should be taken when applying this parameter in a corroding system with addition of inhibitors.

### 3.3 Skew/kurtosis

Other parameters such as skew (or skewness) and kurtosis have been proposed as an alternative for studying corrosion processes [22–25]. However, these properties appear to be influenced by the nature and the frequency of transient corrosion events [26]. Skew and kurtosis are non-dimensional distributions of the EN data [27, 28]. For the skew distribution, a value of zero implies that the distribution is symmetric about the mean; a negative skew implies that there is a tail in the negative direction, and a positive skew implies that there is a tail in the positive direction. For samples taken from a normal distribution (in which the expected skew is zero) the expected standard deviation of the measured skew will be approximately  $\sqrt{6/N}$ , where  $N$ , is the number of points in the recording time. The kurtosis of a distribution is a measure of its flatness. A kurtosis of zero implies that the distribution has a shape similar to the normal distribution. A positive kurtosis implies a more spiky distribution, whereas a negative kurtosis implies a flatter distribution. Kurtosis has a standard deviation considerably larger than the standard deviation of the skew, i.e.,  $\sqrt{24/N}$ .

Figures 7, 8, 9, and 10 show the values of the skew of current and skew of potential skew derived from the on-line monitoring in the solutions S1 and S2 and with addition of the various inhibitors. The results for the solution S1, with and without inhibitor addition, indicate that for the skew, in both, current and potential (Figs. 7 and 8), the measurements show some asymmetry from the average value. For the solution S2 and the various inhibitors, Figs. 9 and 10 show that the values of the skew, in both, current and potential, disclosed larger asymmetry, i.e.,

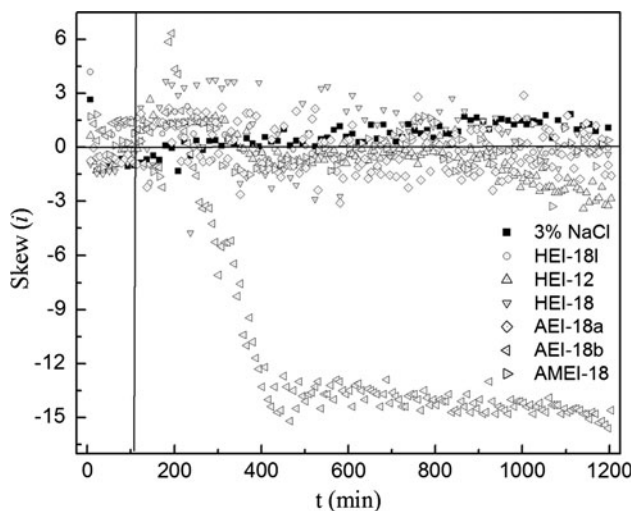


**Fig. 7** Dependence of skew of current as a function of time for 1018 carbon steel exposed to 3% NaCl solution with different types of imidazolines

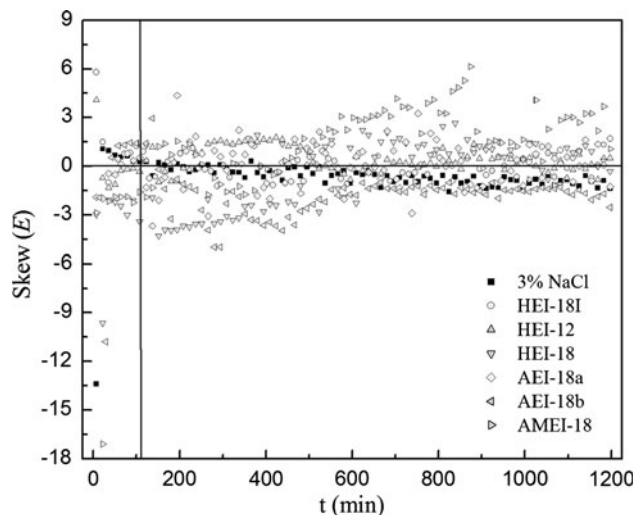


**Fig. 8** Dependence of skew of potential as a function of time for 1018 carbon steel exposed to 3% NaCl solution with different types of imidazolines

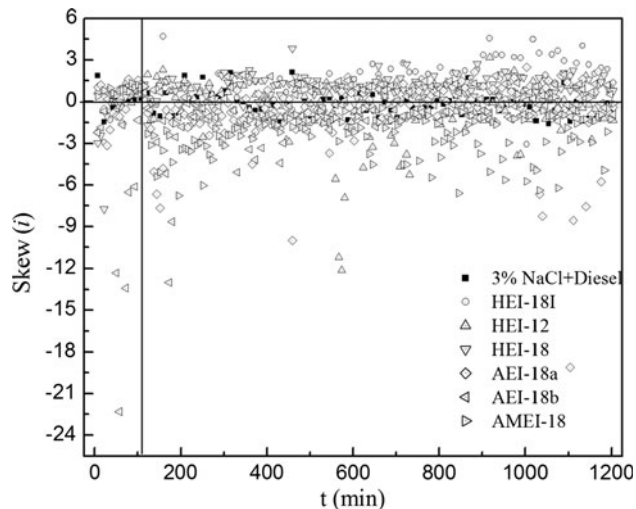


**Fig. 9** Dependence of skew of current as a function of time for 1018 carbon steel exposed to 3% NaCl + diesel solution with different types of imidazolines

larger potential and current fluctuations in both positive and negative directions, as compared with the solution S1. However, it must be taken into account that the calculated standard deviation of skew is for a number of 300 points (data registered by the SmartCET™ equipment) and if we consider that a different value from zero is three times the standard deviation value, then only greater values than 0.42 will indicate asymmetry of the signal. Through this, the signal distribution in the solutions S1 and S2 could be considered symmetric or normal with respect to the media. A particular case is shown by inhibitor AEI-18b, in which the current skew values as a function of time increase (Fig. 7), with no feasible explanation at this stage. The

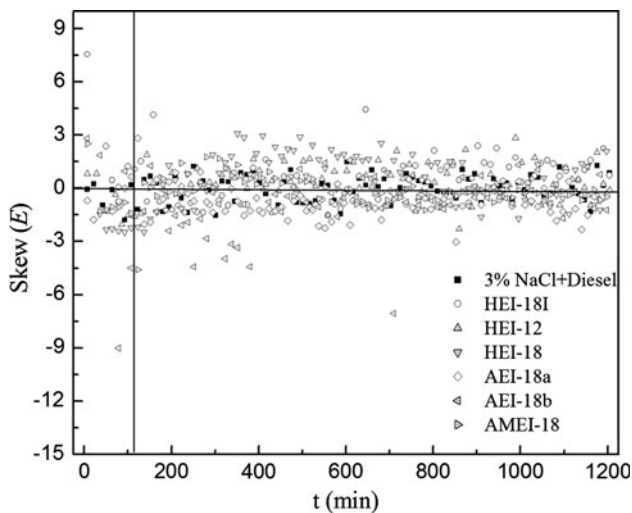


**Fig. 10** Dependence of skew of potential as a function of time for 1018 carbon steel exposed to 3% NaCl + diesel solution with different types of imidazolines

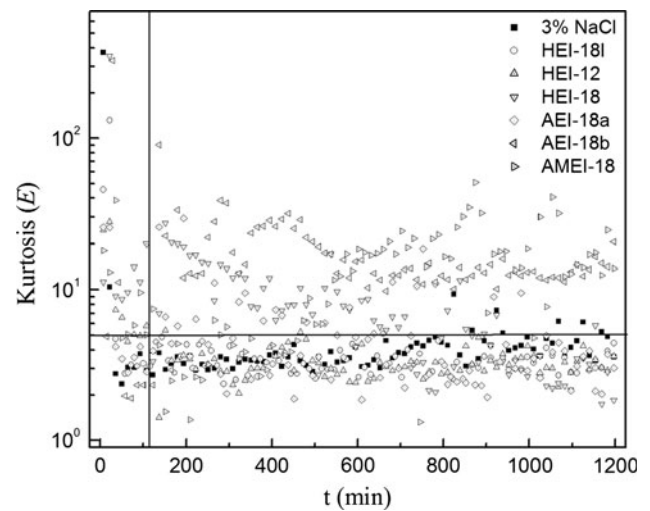


**Fig. 12** Dependence of potential kurtosis as a function of time for 1018 carbon steel exposed to 3% NaCl solution with different types of imidazolines

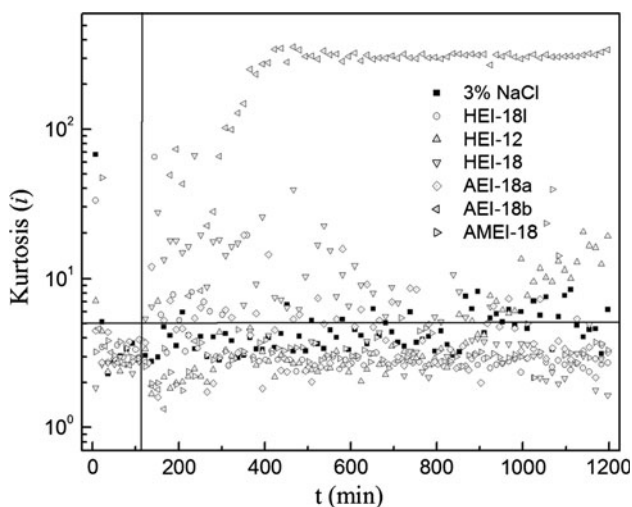


**Fig. 11** Dependence of current kurtosis as a function of time for 1018 carbon steel exposed to 3% NaCl solution with different types of imidazolines

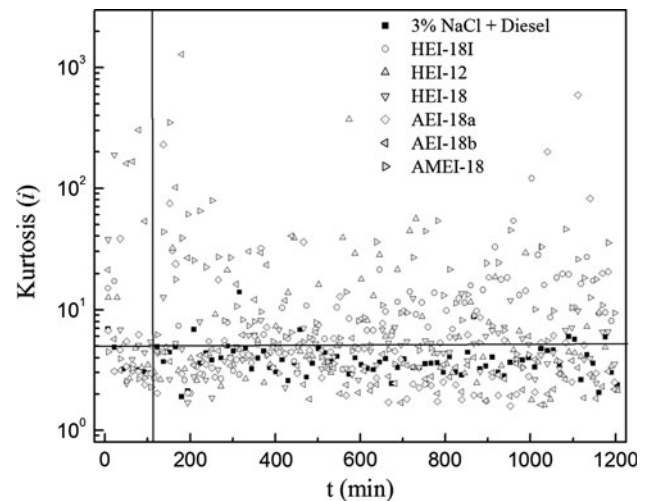


**Fig. 13** Dependence of current kurtosis as a function of time for 1018 carbon steel exposed to 3% NaCl + diesel solution with different types of imidazolines

addition of inhibitors into the solutions S1 and S2 produces greater fluctuations of the skew, in both the current and the potential, in particular for the solution S2. Thus, the skew shows a somewhat similar trend to the one found with the PF (Fig. 12).

The values of kurtosis, in both current and potential, recorded from on-line monitoring in the solutions S1 and S2 and the various inhibitors, are shown in Figs. 11, 12, 13, and 14. In most cases, the measurements in the absence of inhibitors disclosed values around five, which indicate normal distributions, and which can be associated with a uniform corrosion process. It is important to point out, that

in this context, the kurtosis standard deviation (0.84) is twice as that of the skew standard deviation (0.42). The addition of imidazolines in both the solutions leads to variations in the current and the potential kurtosis values, with larger fluctuations (high and low values) in the case of the solution S2, i.e., brine plus oil phase. As with the skew and PF, kurtosis did not show a correlation with the corrosion process observed in this study, which, according to SEM observations, seems to be of uniform nature. In their research of parameter maps (derived from EN) as a technique to discriminate the type of corrosion, Al-Mazeedi and Cottis [29] found that standard deviations of the current and the potential are able to achieve this discrimination, whereas skew and kurtosis do not provide useful

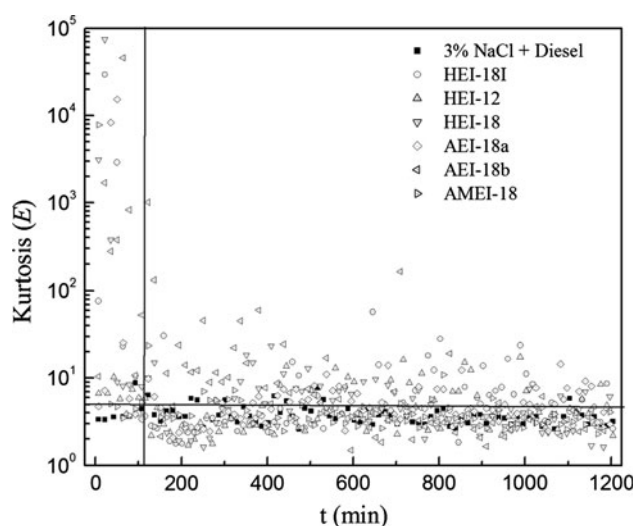


**Fig. 14** Dependence of potential kurtosis as a function of time for 1018 carbon steel exposed to 3% NaCl + diesel solution with different types of imidazolines

discrimination. Nagiub and Mansfeld [30] studied the corrosion behavior of brass with various inhibitors exposed to 3% NaCl and artificial sea water using electrochemical impedance spectroscopy (EIS) and EN. They found that the skew and kurtosis data were very similar in the absence or the presence of inhibitors, whereas the LI did not provide information regarding the corrosion mechanism.

A possible explanation of the high values of parameters such as potential skew and potential kurtosis, could be that these parameters are influenced by the surface polarization of the working electrode, more than the corrosion activities of the solutions, i.e., an inhibited or passive electrode becomes easier to polarize than the one in active condition. Thus, small current fluctuations can lead to higher potential fluctuations, as those recorded in the present research. It is also worthy to note that the skew and the kurtosis can be affected by a possible DC trend from the studied signal. If this trend exists, then it cannot be eliminated because the software processes online data without storing it. It has been recognized that parameters such as skew and kurtosis could give useful indications of the occurrence of localized corrosion for well-defined laboratory conditions [28, 30, 31]. However, under the experimental conditions of the present study, the skew and kurtosis did not show a correlation with the corrosion process observed in this study.

#### 4 Conclusions

1. The results from this study indicate good reliability when different techniques are coupled, i.e., LPR and HA, as a promising method for corrosion rate monitoring,

showing fast response in real-time to small changes in the chemistry of the environment (with or without inhibitors). This allows the acquisition of a number of CR measurements over a short period of time, increasing the reliability and confidence from the data obtained.

2. Traditional LPR technique provides the clearest response and smaller scattering of data in contrast with the more recent HA technique.
3. When assessing inhibitors performance, the values from the PF parameter would erroneously indicate a localized corrosion process. Therefore, special care should be taken when applying this parameter into a corroding system with addition of inhibitors.
4. Statistical parameters such as skew and kurtosis did not show a correlation with the corrosion process observed in this study, at least for the experimental conditions of the present study.

**Acknowledgments** The authors would like to thank the Consejo Nacional de Ciencia y Tecnología (CONACyT), Mexico, for financial support to conduct this study. The authors would also like to express their gratitude to Dr. M. Casales-Díaz for her assistance in this study.

#### References

1. Mok WY, Jenkins AE, Gamble CG (2003) International Conference “Corrosion Science in the 21st Century”, July 2003, paper no., C072, UMIST, Manchester, UK
2. Villamizar W, Magana CS, Chow H et al (2008) CORROSION 2008, paper no. 08286. NACE International, Houston
3. Bosch RE, Bogaerts WF (1996) J Electrochem Soc 143:4033
4. Mészáros L, Mészáros G, Lengyel B (1994) J Electrochem Soc 141:2068
5. Pirnat A, Mészáros L, Lengyel B (1995) Corros Sci 37:963
6. Durmie W, De Marco R, Jefferson A, Kinsella B (2002) Corros Sci 44:1223
7. Gareth J, Rothwell N (2002) CORROSION 2002, paper no., 02337. NACE International, Houston
8. Bell GEC, Rosenthal LM (2000) Lawson, CORROSION 2000, paper no., 00412. NACE International, Houston
9. Teevens J (1998) CORROSION 98, paper no., 388. NACE International, Houston
10. Ryder JC, Pickin NJ, Wooding GP (2001) CORROSION 2001, paper no. 01293. NACE International, Houston
11. Barr EE, Greefiel Pierrard L (2001) CORROSION 2001, paper no. 01288. NACE International, Houston
12. Papavinasam S, Revie RW, Attard M, Demoz A, Michaelian K (2003) Corrosion 59:1096
13. Cottis RA, Al-Awadhi MAA, Al-Mazeedi HA, Turgoose S (2001) Electrochim Acta 46:3665–3674
14. Mansfeld F, Sun Z (1999) Corrosion 55:915–918
15. Sanchez-Amaya JM, Cottis RA, Botana FJ (2005) Corros Sci 47:3280–3299
16. Stern M, Geary L (1957) J Electrochem Soc 104:56
17. Tinnea J, Covino Jr. BS, Bullard SJ et al (2004) CORROSION 2004, paper no. 04435. NACE International, Houston
18. Jovancicevic V, Ramachandran S, Prince P (1999) Corrosion 55:449



19. Villamizar W, Casales M, González-Rodríguez J, Martínez L (2006) *Mater Corros* 57:696
20. Villamizar W, Casales M, González-Rodríguez J, Martínez L (2007) *J Solid State Electrochem* 11:619
21. Kelly RG, Inman ME, Hudson JL (1996) Electrochemical noise measurements for corrosion applications, ASTM SP-1277. In: Kearns JR, Scully JR, Roberge PA et al (eds). ASTM, West Conshohocken
22. Barr EE, Goodfellow R, Rosenthal LM (2000) *CORROSION* 2000, paper no. 414. NACE International, Houston
23. Veilleux B, Lafront AM, Ghali E, Roberge PRJ (2003) *J Appl Electrochem* 33:1093
24. Cappeln F, Bjerrum NJ, Petrushina IM (2005) *J Electrochem Soc* 152:B228
25. Zaveri NN, Sun R, Zufelt N, Zhou A, Chen YQ (2007) *Electrochim Acta* 52:5795
26. Bagley G, Cottis R, Laycock PJ (1999) *CORROSION* 99, paper no. 191. NACE International, Houston
27. Cottis R, Turgoose S (1999) Electrochemical impedance and noise. In: Syrett BC (ed) *Corrosion testing made easy series*. NACE International, Houston
28. Cottis R (2001) *J Corros Sci Eng* 3(4). <http://www.cp.umist.ac.uk/jcse/vol3/Paper4/v3p4.html>
29. Al-Mazeedi HA, Cottis R (2004) *CORROSION* 2004, paper no. 04460. NACE International, Houston
30. Nagiub A, Mansfeld F (2001) *Corros Sci* 43:2147
31. Tristancho JL, Fabian O, Flores LC (2006) IX IBEROMET materials and metallurgy. IberoAmerican Congress, La Habana, pp 144–150